Surface Science 602 (2008) 3018–3025

Contents lists available at ScienceDirect

Surface Science

journal homepage: www.elsevier.com/locate/susc

Time, temperature, and oxygen partial pressure-dependent surface reconstructions on $SrTiO_3(1\,1\,1)$: A systematic study of oxygen-rich conditions ☆

Ann N. Chiaramonti [a,b,*], Courtney H. Lanier [a], Laurence D. Marks [a], Peter C. Stair [c,d]

[a] Department of Materials Science and Engineering, Northwestern University, Evanston, IL, USA
[b] Interfacial Materials Group, Materials Science Division, Argonne National Laboratory, Argonne, IL, USA
[c] Department of Chemistry, Northwestern University, Evanston, IL, USA
[d] Chemical Sciences and Engineering Division, Argonne National Laboratory, Argonne, IL, USA

ARTICLE INFO

Article history:
Received 3 April 2008
Accepted for publication 30 July 2008
Available online 9 August 2008

Keywords:
Transmission high energy electron diffraction
Transmission electron microscopy
Surface reconstruction
Surface structure
Morphology
Roughness and topography
Oxides
Single crystal surfaces

ABSTRACT

The formation of surface reconstructions on the (1 1 1) surface of $SrTiO_3$ following Ar^+ ion bombardment and annealing in oxygen-rich ($0.2 \leqslant pO_2 \leqslant 1.0$) environments is systematically investigated using transmission electron microscopy imaging and diffraction. A series of air stable and highly reproducible reconstructions are observed whose periodicity depends on the combination of annealing time, temperature, and oxygen partial pressure. Approximate phase maps can be constructed for each annealing time investigated, and these reveal that for short annealing times (0.5 h) the periodicity of the observed reconstruction is a primarily function of the partial pressure of oxygen in the annealing environment while for long annealing times (10 h) the observed periodicity is primarily a function of the annealing temperature. For intermediate annealing times (5 h), three coexisting reconstructions are observed to exist on a single specimen.

Published by Elsevier B.V.

1. Introduction

$SrTiO_3$ is a model perovskite of the simplest form, representing one of the most widely studied and well characterized materials systems. $SrTiO_3$ has application in photoelectrolysis [1], as a channel layer in metal-insulator-semiconductor field effect transistors [2], and as a substrate for growth of high T_c superconductors [3], multiferroics [4], and non-volatile random access memory [5]. Additionally, it is often used as a model system for other more complicated perovskites, which are used in heterogeneous catalysis, optoelectronics, and magnetic storage devices.

The structure of bulk $SrTiO_3$ is that of a simple cubic lattice ($a = 3.9$ Å) of strontium with oxygen at the face centers forming an octahedral unit around a body centered titanium. Stacking along [1 1 1] can be described as alternating layers of SrO_3^{4-} and Ti^{4+}, where the subscript denotes the number of atoms in the (1×1) surface unit cell and the superscript denotes the charge on each layer, assuming an ionic model. $SrTiO_3(1\,1\,1)$ is an electrostatically polar surface due to the presence of a non-zero dipole moment in all of the repeat units along [1 1 1] [6]. As such it is inherently unstable in the bulk-like state, as truncating the structure at either the SrO_3^{4-} or Ti^{4+} layer would result in a crystal with diverging electrostatic energy due to the presence of a large macroscopic dipole moment. Nevertheless (1 1 1) surfaces can readily be obtained experimentally, and therefore must be stabilized by some combination of a change in surface stoichiometry, modification of the surface electronic structure, or adsorption of a suitably charged adatom.

A large body of both theoretical and experimental work has focused on the nature of the (0 0 1) and to a lesser extent the (1 1 0) surfaces under a wide range of preparation and treatment conditions, but a comparatively small amount of study has been directed at the (1 1 1) surface. Thus far, this work has consisted primarily of surface morphology, surface unit cell periodicity, and surface electronic structure studies (not atomic-level structure solution). An early electronic structure study by Lo and Somorjai [7] utilizing LEED, AES, and UPS was the first to investigate the effects of Ar^+ ion bombardment and annealing on $SrTiO_3(1\,1\,1)$. It was found that the surface electronic structure and chemical composition depend

* Corresponding author. Address: Interfacial Materials Group, Materials Science Division, Argonne National Laboratory, Argonne, IL, USA. Tel.: +1 630 2525379; fax: +1 630 2524798.
E-mail address: chiaramonti@anl.gov (A.N. Chiaramonti).

0039-6028/$ - see front matter Published by Elsevier B.V.
doi:10.1016/j.susc.2008.07.033

strongly on the annealing and sputtering temperature, and that sputtering at room temperature followed by annealing at 600 °C leads to an Sr-deficient surface with reduced Ti species.

Tanaka and Kawai [8] observed a surface periodicity of $\frac{\sqrt{6}}{2}a$ after annealing for 1 min at 1180 °C in UHV. Following annealing at 1200 °C for 1 min, a structure with periodicity of $(\frac{2}{3})\frac{\sqrt{6}}{2}a$ coexisting with $\frac{\sqrt{6}}{2}a$ was observed, however, this appears to be transient as annealing at 1220 °C again for 1 min in UHV produced a structure with the $\frac{\sqrt{6}}{2}a$ spacing. Based on step height measurements in STM, a bulk-like Ti termination was assigned to the structure annealed at 1220 °C and a bulk-like SrO_{3-x} termination was assigned to the structure annealed at 1180 °C.

In the study by Sigmund et al. [9], specimens were annealed at 950 °C for 2 h in UHV and exhibited LEED patterns with "pronounced 2-fold and weaker 6-fold periodicity". The authors posit based on AES measurements that the surface in this case is Ti terminated.

In an STM/MEIS study by Gömann et al. [10], the authors found that annealing at 1000 °C in UHV conditions for 1 h and in synthetic air produced microfaceted (1×1) surfaces terminated in TiO_2 pyramids. The MEIS showed a broad feature in the band gap corresponding to Ti^+ in the topmost surface layer.

Haruyama et al. [11] found $SrTiO_3(1\,1\,1)$ reduced at 800 °C in UHV exhibited a (1×1) LEED pattern and a clear metallic state in the band gap with a sharp Fermi cut-off. A (4×4) surface structure was obtained after annealing at 1200 °C, and these specimens showed a weakening of the metallic state as well as the occurrence of a localized state approximately 1 eV below E_F. The changes in electronic structure are attributed to modifications of the surface structure with annealing.

Russell and Castell [12] found evidence for coexisting reconstructions with $\left(\sqrt{7} \times \sqrt{7}\right)R19.1^\circ$ and $\left(\sqrt{13} \times \sqrt{13}\right)R13.9^\circ$ periodicity on Nb-doped $SrTiO_3(1\,1\,1)$ annealed in reducing conditions. These surfaces, annealed in UHV at 850 °C for 30 min, are Ti and Sr enriched and O deficient relative to the bulk. In another study, the same authors [13] found surfaces with $(n \times n)$ periodicity, where $\frac{9}{5} \leqslant n \leqslant 6$, following Ar^+ ion sputtering and annealing in UHV and atmospheres up to 4.0×10^{-4} Pa O_2, whereas extended annealing in UHV produced a TiO nanophase surface with a (2×2) unit cell. The authors suggest based on the conditions of formation, that the reconstructions vary in their state of oxidation with the most reduced being the TiO nanophase followed by the (5×5), (6×6), and (4×4), with the most oxidized being the (3×3).

AFM studies of Sekiguchi et al. [14,15] on Nb-doped $SrTiO_3(1\,1\,1)$ found that annealing single crystals at 1000 °C for 10 h in a flow of oxygen resulted in a so-called (1×1) trench structure, where triangular "dents" initially formed (1 h) and then coarsened (5 h) until their sides aligned along a straight line (10 h). In the case of annealing in a flow of argon at 1000 °C for 10 h, a (1×1) structure with a morphology of wide triangular terraces was observed, however, these terraces were observed to be much flatter than those observed following oxygen flow. The structure coarsened with time, and after 5 h the final structure was reached and was proceeding to grow. Following annealing at 1000 °C in air, a complex morphology of self-similar triangles was observed after 5 h. The fractal dimension of these triangles coarsened with time, and the authors conjecture based on the observed morphology that two kinds of nucleation must have occurred on this surface.

Theoretical studies of single crystal $SrTiO_3(1\,1\,1)$ surfaces such as those by Noguera et al. [6,16] focus primarily on electronic structure calculations of (1×1) surfaces, and do not explore large unit cell or non-stoichiometric (defined as any surface that has a stoichiometry different from the bulk) reconstructions. Nevertheless, they find that terminations with various compositions exhibit strong electron redistributions, regardless of whether these surfaces are charge compensated, and that non-stoichiometric surfaces are not necessarily efficient mechanisms for stabilizing the $(1\,1\,1)$ surface.

The focus of this work is to carefully and systematically investigate the structure of the $SrTiO_3(1\,1\,1)$ surface following argon ion bombardment and annealing in oxygen-rich environments using transmission electron microscopy (TEM) techniques as the primary characterization tool. Exact atomic-level surface structure solutions (for example by direct methods applied to transmission electron diffraction data, density functional methods, or scanning tunneling microscopy) will not be discussed here; instead these can instead be found in forthcoming publications by the authors. The intent of this paper is to investigate the phase space of stable, reproducible surface reconstructions on $SrTiO_3(1\,1\,1)$ in oxidizing conditions, namely at 1 atm. of total pressure and with oxygen partial pressures of $0.2 \leqslant pO_2 \leqslant 1.0$.

These pressure regimes have not been studied systematically in the past, so this work is a compliment and extension of the previous UHV and vacuum-based studies. Probing high pressure regimes is relevant to many applications such as heterogeneous catalysis where real reactions often occur at pressures of 1 atm. and above. TEM is uniquely suited to this type of experiment, as it allows for the capture of real and reciprocal space information from the exact same area of a specimen at very high spatial resolution. Because of the transmission geometry and the finite specimen thickness in the direction of the electron beam, TEM is inherently surface sensitive and can probe the bulk, surface, and any buried layers simultaneously in a single experiment.

2. Experimental

Standard TEM specimen preparation methodologies were employed in this study, however, particular care was taken at every stage to ensure the experiments were performed without introducing any foreign species onto the surfaces. This is especially true of any contaminant species which could potentially act as an adatom on the surface of interest. In order to minimize specimen contamination, all glassware, furnace tubes, combustion boats, and hand tools that the crystals came in contact with were thoroughly cleaned prior to use with dilute *aqua regia* followed by a deionized water, acetone, and methanol rinse, and finally a bakeout at 300 °C for 1 h.

High purity (99.9%) single crystals of $SrTiO_3(1\,1\,1)$ were purchased commercially (MTI Corp.) as $10 \times 10 \times 0.5$ mm wafers which were EPI polished on one side. Three millimeter (TEM size) discs were cut from the wafers using a circular disc cutter. The discs were mechanically thinned to approximately 100 μm using SiC polishing paper, and then mechanically dimpled to leave the center approximately 10 μm thick. Only water-based grinding and polishing slurries were used to avoid contamination from oily residues. All specimens were ultrasonically cleaned following the mechanical thinning steps. The discs were perforated to electron transparency following milling for 1–2 h using a Gatan precision ion polishing system (PIPS®) operated at 3–5 keV.

Following Ar^+ ion bombardment at room temperature, $SrTiO_3(1\,1\,1)$ surfaces and near surface regions are non-stoichiometric and Sr deficient [7,17], and amorphous or severely disordered [18]. In order to repair the damage from ion milling and obtain a flat, reconstructed surface, the single crystal TEM-size specimens were annealed at high temperatures in an alumina tube furnace equipped with a high purity gas regulator and flowmeter. The ramp up rate for annealing was 5 °C min^{-1} and the ramp down rate was 8 °C min^{-1}. Dwell times varied from 0.5 to 10 h, at

temperatures from 850 to 1100 °C. The annealing atmospheres consisted of either ambient air, an O_2/N_2 gas mixture, or an O_2/Ar gas mixture, with the gas mixtures used at 1 atm. and 50 sccm flow. The O_2 concentrations of the annealing gas mixtures were varied between 20% and 100%, by volume.

The specimens were examined ex situ at room temperature in one of two transmission electron microscopes: a Hitachi UHV-H9000 operated at 300 kV or a Hitachi H-8100 operated at 200 kV. The procedures for getting quantifiable surface diffraction patterns found in Ref. [19] were followed. Focused probe diffraction, not selected area, was used to identify the presence and periodicity of a surface reconstruction with high spatial precision, while conventional BF/DF imaging was used to study the corresponding morphology and domain structure. HREM analysis was attempted, however, the specimens beam damaged too quickly for the images to provide any additional information. The surfaces in this study were found to be exceptionally air-stable, even surviving for months when stored on a benchtop with no difference in periodicity or obvious change in the intensity ordering of the spots.

3. Results

3.1. As-milled surface

Following Ar^+ ion bombardment, pure $SrTiO_3(1\,1\,1)$ single crystals are under stress and disordered in the near surface region. A bright-field image, Fig. 1, shows bend contours characteristic of a strained thin foil. The corresponding zone-axis diffraction pattern, Fig. 2, shows the bulk diffraction spots allowed for $SrTiO_3(1\,1\,1)$, as well as a diffuse ring around the {1 1 0} spots and an absence of (1×1) spots, both of which are indicators that the near surface region is disordered and devoid of a reconstruction.

3.2. Annealed surfaces

When annealed in ambient air or an O_2/N_2 gas mixture (see Section 2), temperatures greater than 850 °C are required to produce well ordered, flat, and reconstructed surfaces on Ar^+ ion bombarded $SrTiO_3(1\,1\,1)$. The morphology of these surfaces is generally found to be invariant of the actual reconstruction, however, it does appear to depend to a small degree on the specimen miscut and total ion milling time. Terraces are observed to coarsen with higher temperatures and longer annealing times. Similar to the (0 0 1) and (1 1 0) surfaces, the (1 1 1) surface of $SrTiO_3$ (Fig. 3) exhibits large, flat, often triangular terraces separated by step bunches. The TEM specimens typically show microfacets along the specimen/vacuum edge (the upper right corner of Fig. 3). These microfacets and step bunches are oriented primarily along the ⟨1 1 0⟩ directions. The specimens also often contain screw dislocations intersecting the plane of the foil, which are an artifact of the

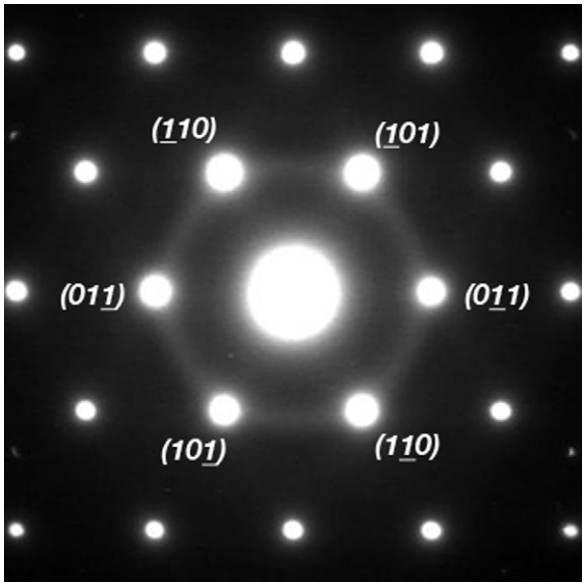

Fig. 2. Transmission electron diffraction pattern of an as-milled (1 1 1) surface along the [1 1 1] zone axis. A diffuse ring around the {1 1 0}-type spots and the absence of (1×1) spots indicates that the near surface region is disordered.

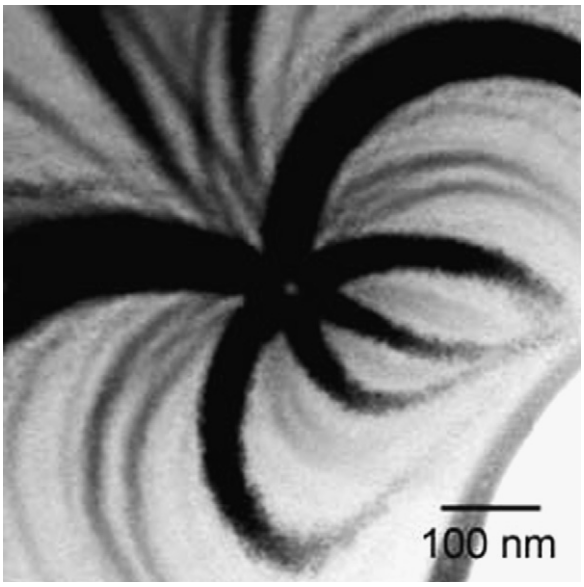

Fig. 1. Bright-field TEM image of an as-milled (1 1 1) surface. The image shows extinction contrast which is indicative of local strain or bending. Such "bend contours" are observed in the electron transparent regions of the specimen around the ion mill perforation.

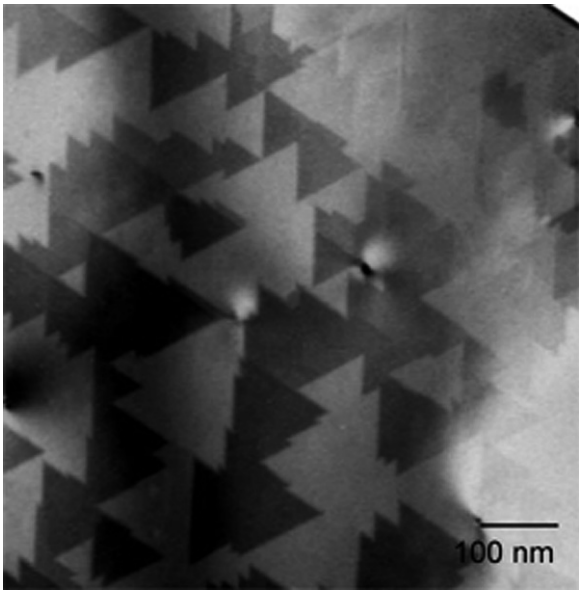

Fig. 3. Bright-field TEM image of $SrTiO_3(1\,1\,1)$ following annealing in air for 5 h at 1050 °C. The image shows a flat surface with triangular terraces and step bunches aligned along ⟨1 1 0⟩ directions. Several screw dislocations can be seen intersecting the surface of the foil. The specimen edge/vacuum interface is in the upper right corner of the image.

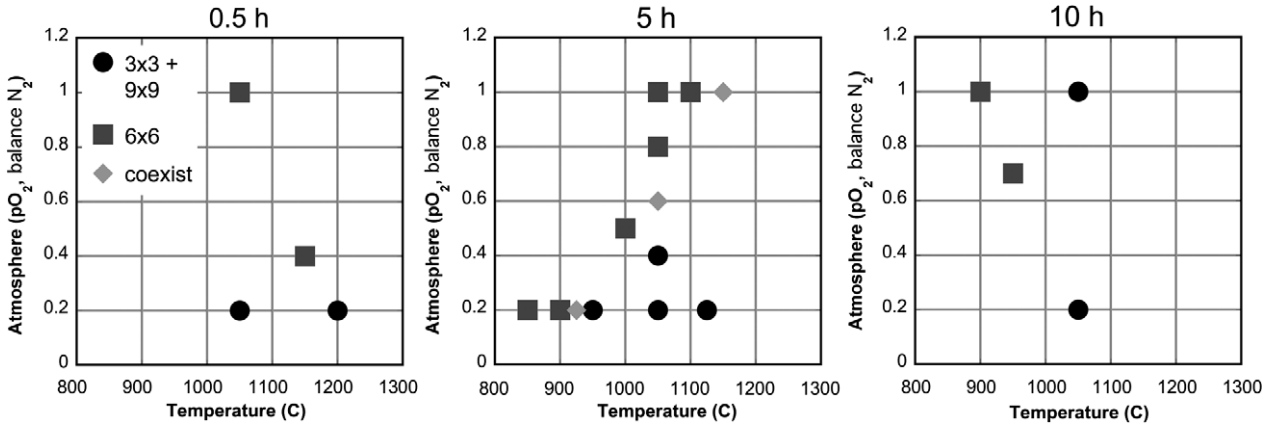

Fig. 4. Experimental phase maps for 0.5, 5, and 10 h anneals plotted as a function of annealing temperature and oxygen partial pressure. The (6×6) surface reconstruction is denoted in squares, the $(3 \times 3) + (9 \times 9)$ phases as circles, and the coexistence of all three phases is denoted by diamonds and was observed only upon annealing for 5 h.

specimen preparation process and also observed on $SrTiO_3(001)$ and (110) surfaces [20,21].

Fig. 4 is a graphical summary of the current annealing results. This figure shows the surface reconstructions obtained for various combinations of annealing time ($0.5 \leqslant t \leqslant 10$ h), temperature ($850\ ^\circ C \leqslant T \leqslant 1100\ ^\circ C$), and oxygen partial pressure ($0.2 \leqslant pO_2 \leqslant 1.0$). The following points should be noted:

- A family of $n \times n$ reconstructions is observed, where $n = 3, 6, 9$.
- The surface reconstruction observed is a function of annealing time, temperature, and oxygen partial pressure.
- Under certain annealing conditions, several reconstructions coexist on the specimen at the same time.
- The (3×3) diffraction spots always coexist with another set of spots having (9×9) periodicity.

The subsequent sections are devoted to discussing the properties of the individual surfaces observed in this study.

3.2.1. (6×6)

Transmission electron diffraction patterns from specimens annealed for short times at high oxygen partial pressure or for long times at lower temperatures have spots with (6×6) periodicity, corresponding to a 33.1 Å unit cell. The diffraction pattern characteristic of these surfaces is shown in Fig. 5, where the bulk {110}-type spots can be seen along with the (6×6) periodic surface spots. A dark-field image of this surface exhibiting a large area of well ordered (6×6) domains is shown in Fig. 6.

3.2.2. $(3 \times 3) + (9 \times 9)$

Transmission electron diffraction patterns from specimens annealed for short times at lower oxygen partial pressures or for long times at higher temperatures have spots corresponding to two different surface unit cells: one having (3×3) periodicity with a 16.6 Å unit cell, and another having (9×9) periodicity with a 49.7 Å unit cell. This diffraction pattern is shown in Fig. 7. The (9×9) surface reconstruction has a prominent (5×5) modulation, and could alternatively be indexed as a $(\frac{9}{5} \times \frac{9}{5})$ reconstruction with a 9.9 Å unit cell. However, it is much simpler and more intuitive to refer to the structure as a (9×9), so this will be the convention throughout this paper.

For all of the annealing conditions explored in this study, specimens whose diffraction patterns have the (3×3) diffraction spots also have the (9×9) spots. There has never been a case where one set of spots was observed independent of the other. While it is possible that all of the spots correspond to a single reconstruction, the intensity ordering of the spots as well as the fact that (3×3) domains are readily imaged in dark-field indicates that the diffraction pattern consists of two sets of spots, each corresponding to a different surface reconstruction. The studies of Sekiguchi et al. [14,15] used nearly the same annealing conditions and support this conclusion, as it was found that annealing in air for 5 h produced surfaces "where two kinds of nucleation must have occurred".

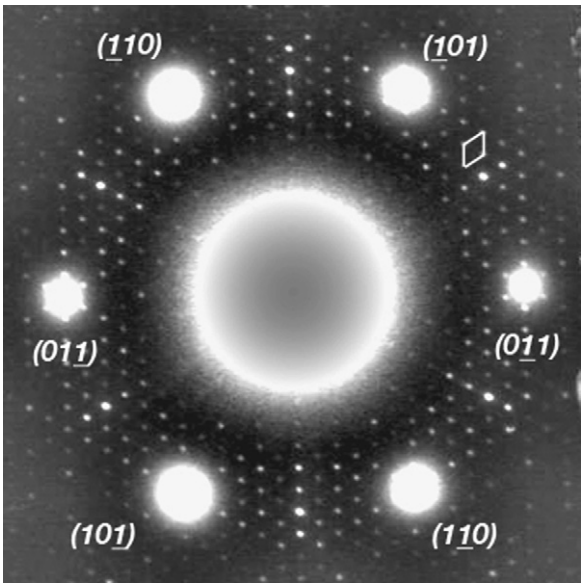

Fig. 5. Transmission electron diffraction pattern of the $SrTiO_3(111)$-6×6 reconstruction; a (6×6) unit cell is denoted.

3.3. Coexisting (6×6), (3×3), and (9×9)

As seen in Fig. 4, there are several instances where annealing at a particular combination of temperature, oxygen partial pressure, and time will yield a specimen whose transmission electron diffraction pattern (Fig. 8) has three distinct sets of spots corresponding to three coexisting surface reconstructions.

Although the intensity ordering of the spots and their systematic presence and/or absence indicates that there are three distinct surface reconstructions on this particular specimen, the domains were imaged individually in dark-field to rule out the possibility of a supercell. Fig. 9a is a dark-field TEM image of a specimen annealed at 1050 °C for 5 h in 50 sccm flow of 60% oxy-

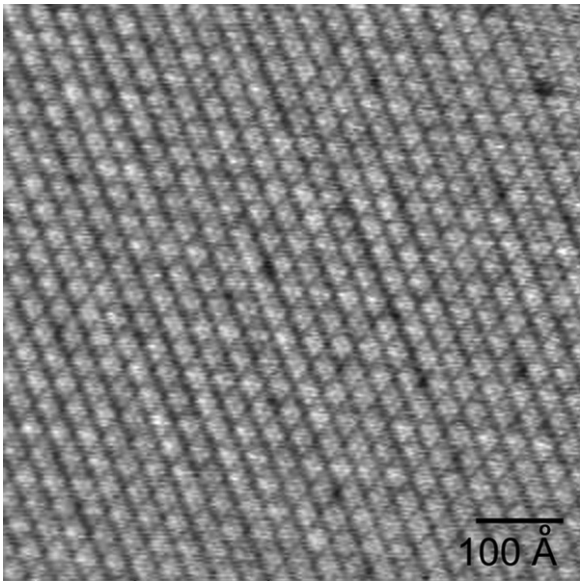

Fig. 6. Dark-field TEM image of the (6 × 6) surface showing a large area of well ordered domains.

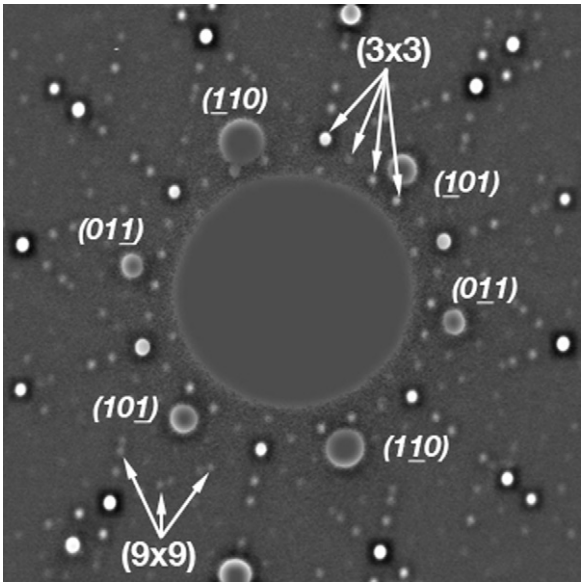

Fig. 7. $SrTiO_3$(111)-3 × 3 surface diffraction pattern. Arrowed are spots corresponding to both the (3 × 3) and (9 × 9) surface reconstructions. This image has been high-pass filtered to enhance the contrast of the weak surface spots.

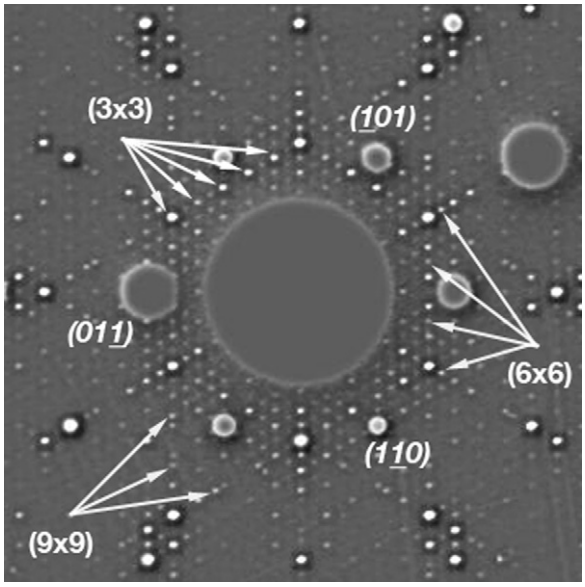

Fig. 8. TEM diffraction pattern showing bulk allowed, (6 × 6), (3 × 3), and (9 × 9) periodic spots coexisting on a single specimen. The image has been high-pass filtered to enhance contrast of the weak diffraction spots.

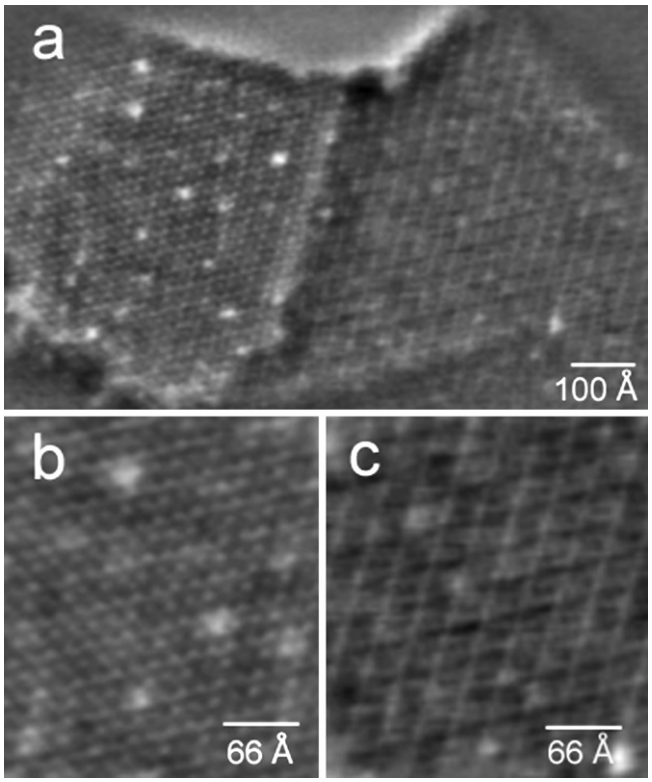

Fig. 9. (a) Dark-field TEM image of neighboring (3 × 3) and (6 × 6) domains. (b) Magnified view of the left side (3 × 3) domain. (c) Magnified view of the right side (6 × 6) domain. In order to remove random (shot) noise and enhance the quality of the image, a soft circular mask was applied followed by a Wiener filter.

gen/40% argon, and whose diffraction pattern is similar to that shown in Fig. 8.

The dark-field image shows two domains with different periodicity coexisting next to each other, thus ruling out a large supercell. Fig. 9b is an enlargement of the left domain, and resolves the 16.6 Å (3 × 3) lattice. Similarly, Fig. 9c is an enlargement of the right domain, and clearly resolves the 33.1 Å (6 × 6) lattice. From Fig. 9a, the size of each domain is approximately 50 nm × 50 nm, although this is likely a minimum number as the edge of a domain is difficult to distinguish because the transmission geometry precludes distinguishing a domain boundary on the top surface from one on the bottom. A domain corresponding to the (9 × 9) surface reconstruction is not observed in the experimental image (however, the spots are present in the diffraction pattern). One explanation for the lack of experimental image of the (9 × 9) surface reconstruction is that the dark-field technique, tilt condition, and objective aperture used to obtain the image in Fig. 9 is not appropriate for simultaneously imaging all three reconstructions present. Another option is that the (9 × 9) recon-

struction exists only in small areas of the specimen, for example near step edges or at other high energy sites.

4. Discussion

The formation of surface reconstructions on Ar^+ ion milled and annealed $SrTiO_3(1\,1\,1)$ is complex and occurs under the influence of many competing factors. One factor is that the (1 1 1) is a polar surface [22], meaning reconstructions that form must be valence compensated in order to cancel the macroscopic component of the dipole moment either by charge transfer, adatom adsorption, changes in stoichiometry, or a combination of these. Next, Ar^+ ion milling, both the kind used for TEM sample preparation and for surface science sample cleaning, can be destructive to both the structure and stoichiometry of the surface and near surface region. Reconstructions that form after ion milling must overcome a high degree of structural disorder and incorporate a large number of point defects such as vacancies, interstitials, and antisites. For a typical TEM sample whose thickness is in the range of 25–100 nm, this implies that the regions being examined may contain a large fraction of material that has interacted with the ion beam. The study of $SrTiO_3(1\,1\,1)$ is further complicated by the fact that experimental evidence indicates that many of the observed surface reconstructions have very similar energies and compositions, since they have been observed to coexist on a single specimen under a wide range of pre-treatments, temperatures, and annealing atmospheres.

The annealing data indicates that for short annealing times (0.5 h), the periodicity of the observed reconstruction is mainly a function of the oxygen partial pressure in the environment whereas for long annealing times (10 h), the periodicity of the observed reconstruction is mainly a function of the annealing temperature. The data for the intermediate annealing condition (5 h) is a mix of the two: the reconstruction observed is a function of both the annealing atmosphere and the temperature. For pure undoped single crystals treated in oxidizing environments, it is proposed that an observed reconstruction forms by the action of two processes: partial re-oxidation of the surface and bulk self-diffusion.

Prior to annealing, the surface and selvedge of Ar^+ ion milled $SrTiO_3(1\,1\,1)$ are structurally disordered and slightly reduced. They will contain ionic and point defects such as isolated vacancies and interstitials, antisites, and Schottky and Frenkel pairs, present intrinsically and also formed by the action of ion milling [23–28]. It has been shown previously that oxygen is preferentially removed by ion milling [7,28,17], so the surface and selvedge will contain a large number of highly mobile [29,26,30] defects such as oxygen vacancies. When oxygen vacancies are present at the surface, they serve as ready sites for gas phase molecular oxygen, either physisorbed or chemisorbed on the surface, to dissociate and incorporate into the lattice, for example via the exchange $\frac{1}{2}O_2(g) + V_0'' \rightleftharpoons O_0 + 2h^{\cdot}$. This reaction has been shown to have a low enthalpy [25], and is the pathway for the initial (re)oxidation of the selvedge, which occurs rapidly as reconstructions are observed to form in as little as 0.5 h in this work. Oxidation of reduced bulk $SrTiO_3$ has been shown to occur at times as short at 1 h for reduced Verneuil-grown bulk single crystals [30], and it is reasonable to expect that re-oxidation of the surface and selvedge in a TEM specimen with a total thickness of 25–100 nm in the presence of gas phase oxygen could occur in even shorter times. The rate of re-oxidation depends on both the concentration of molecular oxygen available to the surface, e.g. the gas phase oxygen partial pressure in the annealing environment, and on the concentration of surface defects serving as ready adsorption and dissociation sites for molecular oxygen. While bulk self-diffusion is a factor, it is a secondary effect for the shorter annealing times because the concentration of surface defects resulting from Ar^+ bombardment is initially very high. Upon annealing for $0.5\ \text{h} \leqslant t \leqslant 5\ \text{h}$, the concentration of point defects decreases as the surface becomes increasingly ordered.

The 5 h annealing times in this study are an intermediate between the surface defect mediated regime, where gas phase oxygen is readily dissociated at the surface and incorporated into the selvedge, and the bulk diffusion-mediated regime, where intrinsic point defects can move to and from the surface and recombine or annihilate as dictated by thermodynamics. Since oxygen and strontium defects are more mobile than Ti defects [28], and neutral SrO Schottky defects are known to be low energy defects in $SrTiO_3$ [27], strontium vacancy diffusion is almost certainly also important. After annealing for 5 h, the surface point defects generated by ion milling are lower in number because of partial re-oxidation, however, the numbers of intrinsic point defects in the bulk and selvedge as well as structural defects at the surface are increasing as the surface fully orders and begins to coarsen. The structural defects, which have all been observed on annealed specimens in this study, could also serve as molecular oxygen adsorption/dissociation sites and include dislocations, jogs and kinks, terrace edges, surface faceting, and step bunches. It is in this intermediate timeframe that coexisting reconstructions (for example those in Fig. 8) are observed.

For the longest annealing times of 10 h, the periodicities of the reconstructions observed in this study are solely a function of annealing temperature, as seen in Fig. 4c, whereas initially the partial pressure of oxygen in the annealing atmosphere dominates the formation of reconstructions by simply making immediately available to the large number of surface defect sites more or less oxygen to be dissociated at the surface and incorporated into the surface and selvedge, once the surface and selvedge have partially or fully re-oxidized, the relatively small range of partial pressures explored here, which do not even vary by an order of magnitude, are not large enough to compete with the effect of temperature driving the system toward thermodynamic equilibrium by self-diffusion and reaction of intrinsic point defects, for example $V_{Sr}'' + V_O^{\cdot\cdot} \rightleftharpoons [V_{Sr}'' : V_O^{\cdot\cdot}]^x$ or $Sr_{Sr}^x + Ti_{Ti}^x + 3O_O^x + [V_{Sr}'' : V_O^{\cdot\cdot}]^x \rightleftharpoons TiO_2$. The possibility that a small amount of gas phase oxygen still comes into the lattice at a few structural defect sites and then diffuses through the bulk of the crystal, analogous to the Mars-Van Krevelen reaction mechanism in heterogeneous catalysis, cannot be completely ruled out.

There is at least one report in the literature on the formation of similarly indexed reconstructions ($n \times n$, where $n = 3,6$) on $SrTiO_3(1\,1\,1)$ following Ar^+ ion bombardment and annealing in vacuum and UHV [13]. In that case, the crystals were Nb-doped. Despite the fact that the contribution of the Nb to the surface thermodynamics and kinetics cannot be ignored, as Nb doping introduces both crystallographic and electronic (band structure) changes to the crystal, one can suggest a mechanism for the formation of reconstructions in vacuum that is independent of the action of dopants. Ar^+ ion milled specimens annealed in oxygen-poor environments cannot partially re-oxidize the surface and selvedge by the incorporation of gas phase oxygen in the same way as specimens annealed in oxygen-rich environments. Upon heating in vacuum, sputtered surfaces can, however, partially re-oxidize the surface and selvedge by the action of self-diffusion exchange with the bulk in a process analogous to the bulk-assisted re-oxidation that is well known to occur on the surface of rutile (TiO_2), the driving force for mass transport being the concentration gradient that exists between the sputter reduced selvedge and the bulk. This process involves little if any reduction by mass exchange with the vacuum, since the crystals are already slightly reduced from ion milling.

While it is at first glance counterintuitive that vacuum annealing can re-oxidize surfaces, it is widely accepted to occur in the rutile system [31] and does offer a plausible explanation as to why sputtered surfaces annealed in vacuum have reconstructions with the same periodicities to those observed in this study, whereas stoichiometric surfaces (cleaved or polished but not sputtered) show periodicities that are different than those observed in this study. Clean stoichiometric surfaces are not reduced and do not initially have a concentration gradient, thus there is no basis and no driving force for bulk-assisted re-oxidation. Instead, upon vacuum annealing these will immediately undergo a reduction [29,24,26,27,23] and surface reconstructions will form which are likely to be different from those observed after a re-oxidation process since they started from different initial stoichiometries. Since the crystals used in the studies of Ref. [13] are thicker than the TEM specimens examined in this work by at least several orders of magnitude, the bulk can serve as a ready and nearly infinite source of atoms for bulk self-diffusion in oxygen-poor conditions where oxygen incorporation from the gas phase at surface defect sites is not possible. Regardless of the initial stoichiometry of the selvedge (e.g. ion milled or not), given a sufficient period of time an equilibrium surface composition should eventually be reached that is dependent only on the overall thermodynamics of the system, for example the chemical potential of oxygen in the annealing environment, the temperature, and whether it is an open or closed system.

5. Conclusions

Several air-stable and highly reproducible surface reconstructions have been observed to form on 25–100 nm thick Ar^+ ion milled TEM specimens of $SrTiO_3$(1 1 1) upon annealing in oxidizing environments. TEM-type specimens are not required, however, as these reconstructions have been prepared on bulk single crystals and could equally well be produced on thin films by following the annealing recipes (time, temperature, pO_2) described herein, noting that total annealing times may be less for specimens that have not been ion milled.

The exact reconstruction that forms upon annealing depends on a combination of the annealing atmosphere, time, and temperature. For the shortest annealing times of 0.5 h, the observed reconstruction is primarily a function of the oxygen partial pressure in the annealing atmosphere. For the longest annealing times of 10 h, the observed reconstruction is a primarily a function of the annealing temperature. For intermediate annealing times, the surface reconstruction formed is a strong function of both the annealing temperature and oxygen partial pressure. It is under the intermediate annealing times that three coexisting reconstructions have been observed. The atomic-level structure of the $(n \times n)$ surfaces, as well as a more complete analysis of the basic (1×1) structural motifs for the (1 1 1) surface will be the topic of future publications.

While it is interesting to compare the current results with previous surface science studies of the (1 1 1) surface of $SrTiO_3$, care should be taken as the degree of ion milling needed to perforate a thin foil for TEM examination can sometimes be more than that typically employed in cleaning specimens for surface science analysis. In other words, the initial degree of non-stoichiometry at the selvedge may be high compared to other studies implying that longer annealing times may be required to reach a given composition. Also, because the total thickness of a TEM specimen is 25–100 nm, the relative volume of surface and selvedge to bulk is high, which may be different from studies where a bulk single crystal is used. Finally one must carefully consider the effect of doping on the overall defect chemistry of the system [32].

These results show that several different air stable reconstructions with an extremely high degree of reproducibility can be prepared on the (1 1 1) polar surface of $SrTiO_3$ with a wide range of variance in unit cell size and by extension, atomic and electronic structure. As $SrTiO_3$ is used as a substrate for the growth of a host of materials ranging from superconductors to multiferroics, these reconstructions may hold the key to fostering interesting and novel surface and interface phenomena. One example is the reversible resistive switching observed in $SrTiO_3$ [33], where the interface between the oxide and the metal electrode is believed to play a critical role in controlling the switching behavior. If the $SrTiO_3$ surface is engineered to have a specific reconstruction, which implies a specific atomic and more importantly electronic structure different from the bulk, it may be possible to tune or alter the current–voltage characteristics. Another example is the case of extrinsic magnetoelectronic coupling, which has been calculated to occur at the interface between $SrTiO_3$ and $SrRuO_3$ [34]. The magnetoelectric response of such a multilayer is determined by the complex interrelation between the atomic structure, chemistry, electronic structure, and nature of the bonding at the interface, all of which could vary if the surface of the $SrTiO_3$ in contact with the $SrRuO_3$ was reconstructed.

Acknowledgements

The authors would like to acknowledge the contributions of W. Tu and J.-Y. Kim to the TEM specimen preparation and annealing.

This work was supported by the EMSI program of the National Science Foundation and the US Department of Energy Office of Science (CHE-9810378) as well as the Chemical Sciences, Geosciences, and Biosciences Division of the Office of Basic Energy Sciences, Office of Science, US Department of Energy (DE-FG02-03ER15457) at the Northwestern University Institute for Environmental Catalysis. Argonne National Laboratory, a US Department of Energy Office of Science Laboratory, is operated under Contract No. DE-AC02-06CH11357.

References

[1] M.S. Wrighton, P.T. Wolczanski, A.B. Ellis, Journal of Solid State Chemistry 22 (1977) 17.
[2] K. Shibuya, T. Ohnishi, T. Lippmaa, M. Kawaskai, H. Koinuma, Applied Physics Letters 85 (2004) 425.
[3] V. Agrawal, N. Chandrasekhar, Y.J. Zhang, V.S. Achutharaman, M.L. McCartney, A.M. Goldman, Journal of Vacuum Science and Technology A 10 (1992) 1531.
[4] X. Marti, F. Sanchez, J. Fontcuberta, M.V. Garcia-Cuenca, C. Ferrater, M. Varela, Journal of Applied Physics 99 (2006) 08P302.
[5] M.A. Zurbuchen, J. Lettieri, Y. Jia, D.G. Schlom, S.K. Streiffer, M.E. Hawley, Journal of Materials Research 16 (2001) 489.
[6] A. Pojani, F. Finocchi, C. Noguera, Surface Science 442 (1999) 179.
[7] W.J. Lo, G.A. Somorjai, Physical Review B 17 (1978) 4942.
[8] H. Tanaka, T. Kawai, Surface Science 365 (1996) 437.
[9] W.M. Sigmund, M. Rotov, Q.D. Jiang, J. Brunen, J. Zegenhagen, F. Aldinger, Applied Physics A 64 (1997) 219.
[10] A. Gömann, K. Gömann, M. Frerichs, V. Kempter, G. Borchardt, W. Maus-Friedrichs, Applied Surface Science 7 (2005) 2053.
[11] Y. Haruyama, Y. Aiura, H. Bando, Y. Nishihara, H. Kato, Journal of Electron Spectroscopy and Related Phenomena 88 (1998) 695.
[12] B.C. Russell, M.R. Castell, Physical Review B 75 (2007) 155433:1.
[13] B.C. Russell, M.R. Castell, Journal of Physical Chemistry C 112 (2008) 6538.
[14] S. Sekiguchi, M. Fujimoto, M. Kang, S. Koizumi, S. Cho, J. Tanaka, Japanese Journal of Applied Physics 37 (1998) 4140.
[15] S. Sekiguchi, M. Fujimoto, M. Nomura, S. Cho, J. Tanaka, T. Nishihara, M. Khang, P. Hyong-Ho, Solid State Ionics 108 (1998) 73.
[16] A. Pojani, F. Finocchi, C. Noguera, Applied Surface Science 142 (1999) 177.
[17] Y. Adachi, S. Kohiki, K. Wagatsuma, M. Oku, Applied Surface Science 143 (1999) 272.
[18] A.N. Chiaramonti, Structure and Thermodynamics of Model Catalytic Oxide Surfaces, Ph.D. Thesis, Northwestern University, Evanston, IL 60208, December 2005.
[19] A.N. Chiaramonti, L.D. Marks, Journal of Materials Research 20 (2005) 1619.
[20] N. Erdman, K.R. Poeppelmeier, M. Asta, O. Warschkow, D.E. Ellis, L.D. Marks, Nature 419 (2002) 55.

[21] A.K. Subramanian, Transmission Electron Microscopy Studies of Surface Phenomena in Polar Oxides, Ph.D. Thesis, Northwestern University, Evanston, IL 60208, June 2005.
[22] C. Noguera, F. Finocchi, J. Goniakowski, Journal of Physics: Condensed Matter 16 (2004) S2509.
[23] L.C. Walters, R.E. Grace, Journal of Physics and Chemistry of Solids 28 (1967) 239.
[24] H. Yamada, G.R. Miller, Journal of Solid State Chemistry 6 (1973) 169.
[25] N.G. Eror, U. Balachandran, Journal of Solid State Chemistry 42 (1982) 227.
[26] J. Crawford, P. Jacobs, Journal of Solid State Chemistry 144 (1999) 423.
[27] T. Tanaka, K. Matsunaga, Y. Ikuhara, T. Yamamoto, Physical Review B 68 (2003) 205213.
[28] B.S. Thomas, N.A. Marks, B.D. Begg, Nuclear Instruments and Methods in Physics Research B 254 (2007) 211.
[29] L.C. Walters, R.E. Grace, Journal of Physics and Chemistry of Solids 28 (1967) 245.
[30] A.E. Paladino, L.G. Rubin, J.S. Waugh, Journal of Physics and Chemistry of Solids 26 (1965) 391.
[31] M.A. Henderson, Surface Science 419 (1999) 174.
[32] R. Meyer, R. Waser, J. Helmbold, G. Borchardt, Journal of Electroceramics 9 (2002) 101.
[33] K. Szot, W. Speier, G. Bihlmayer, R. Waser, Nature Materials 5 (2006) 312.
[34] J.M. Rondinelli, M. Stengel, N.A. Spaldin, Nature Nanotechnology 3 (2008) 46.